DOI: 10.1002/chem.200801240

Passage from Stepwise to Concerted Dissociative Electron Transfer through Modulation of Electronic States Coupling

Cyrille Costentin,* Ludovic Donati, and Marc Robert*[a]

Abstract: Reductive cleavage of the three cyanobenzyl chloride isomers in *N*,*N*-dimethylformamide gives new insights into the factors that control the mechanism during dissociative electron transfer. Within the family of investigated compounds, electrochemical reduction leads to expulsion of the chloride ion. While electron transfer is concerted with breaking of the C–Cl bond and acts as the rate-determining step in the case of both the *ortho* and *para* isomers, an intermediate anion radical is formed before rapid fragmentation in the case of the *meta* isomer. Such an unexpected mechanistic shift (all key thermodynamic parameters are very similar for the three chlorides) is interpreted in the framework of a modified version of the dissociative electron-transfer model that includes electronic coupling effects between the diabatic states of the products. These effects appear to control the very existence of a transient species along the reaction pathway.

Keywords: cyanobenzyl chlorides · electrochemistry · electron transfer · radical ions · reaction mechanisms

Introduction

Coupling between electron transfer and bond breaking may involve competitive concerted and stepwise pathways, as shown schematically in Scheme 1 and in terms of potential-energy profiles in Figure 1.[1] If the intermediate anion radical "does not exist", that is, lives for less than a vibration, the concerted pathway is necessarily followed. If the intermediate exists, the stepwise pathway is not necessarily followed.

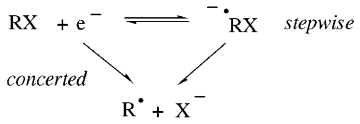

e⁻ : *electrode, homogeneous (ground state, excited state)*

Scheme 1. Concerted and stepwise pathways for dissociative electron transfer.

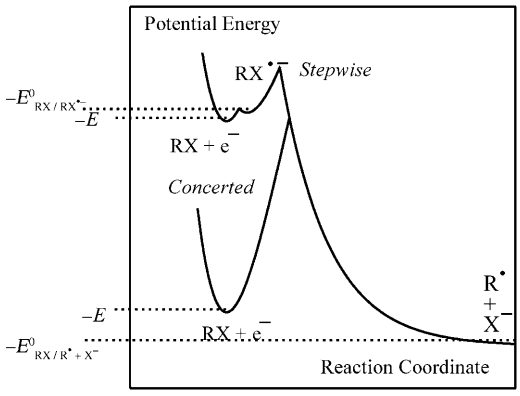

Figure 1. Potential-energy profiles for the concerted and stepwise pathways according to Scheme 1. The E^0 are the standard potentials of the subscript couples. E is the electrode potential or the standard potential of the homogeneous donor.[2]

The reaction proceeds through the most energetically favorable path in Figure 1. Competition between the two routes hinges on structural factors that are related to the four terms in the expression of the standard free energy for cleavage of the intermediate anion radical [Eq. (1)]

$$\Delta G^0_{^{-\bullet}RX\rightarrow R^\bullet + X^-} = D_{RX\rightarrow R\bullet + X\bullet} - T\Delta S_{RX\rightarrow R\bullet + X\bullet} + E^0_{RX/^{-\bullet}RX} - E^0_{X^\bullet/X^-} \quad (1)$$

[a] Prof. Dr. C. Costentin, L. Donati, Prof. Dr. M. Robert
Laboratoire d'Electrochimie Moléculaire
UMR 7591 CNRS, Université Paris Diderot (Paris 7)
15 rue Jean de Baif 75205, Paris Cedex 13 (France)
Fax: (+33) 1-47278791
E-mail: cyrille.costentin@univ-paris-diderot.fr
robert@univ-paris-diderot.fr

Supporting information for this article is available on the WWW under http://dx.doi.org/10.1002/chem200801240.

where $D_{RX\rightarrow R^{\cdot}+X^{\cdot}}$ is the homolytic bond-dissociation energy of RX, $\Delta S_{RX\rightarrow R^{\cdot}+X^{\cdot}}$ the corresponding entropy change, and $E^0_{RX/^{-}\cdot RX}$ and $E^0_{X^{\cdot}/X^{-}}$ are the standard potentials of the subscript couples (energies in electron volts, potentials in volts). The more negative $\Delta G^0_{^{-}\cdot RX\rightarrow R^{\cdot}+X^{-}}$, the more favorable the concerted pathway, and vice versa.

The outcome of the competition also depends on the driving force offered by the electron donor. As represented in Figure 1 by a vertical upward translation of the reactant curve, a strong reducing agent favors the stepwise route, and vice versa. Thus, in borderline situations, the system may pass from one mechanism to the other on variation of the electrode potential or the standard potential of the homogeneous electron donor,[3] and this possibly results in systems that undergo concerted electrochemical and stepwise photoinduced electron-transfer reactions.[4]

The classical Marcus–Hush model of outer-sphere electron transfer[5] is applicable to the electron-transfer step of the stepwise reaction, whereas Morse-curve models can be used for the concerted pathway[6] and for cleavage of the intermediate radical anion in the stepwise case.[7] All three reactions are characterized by a quadratic activation/driving force relationship. In each case the intrinsic barrier may be expressed by means of parameters involving the reactant and product states, the main component of which is the bond dissociation energy for the two bond-breaking reactions. Radical anion cleavage may be heterolytic [as shown in Scheme 1 and Eq. (1)] or homolytic ($^{-}\cdot RX\rightarrow R^{-}+X^{\cdot}$).[1a,8] In the heterolytic case,[1d,7,9] but also in the homolytic case,[10] it can be viewed as an intramolecular dissociative electron-transfer reaction.

These mechanistic analyses have been improved by consideration of the interactions that may exist between the caged fragments resulting from cleavage, which leads to what can be alternatively called a σ ion radical (Scheme 2).[11a] There are definite clues that these adducts may survive in polar solvents, albeit considerably weakened as compared to their gas-phase counterparts.[11b] The corresponding potential-energy profiles are shown in Figure 2.

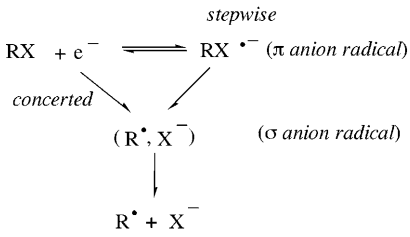

Scheme 2. Sticky dissociative electron transfer.

Quadratic activation/driving force relationships are still found, but with diminished contributions of the bond-dissociation energies.[11a,12] The stability of the σ anion radical adduct varies with the nature of the solvent. It decreases with increasing ability of the solvent to solvate the leaving group.[11b] The purpose of the present paper is to discuss the influence of molecular structure on the concerted versus stepwise dichotomy and on the very existence of an intermediate ion radical in the family of the cyanobenzyl chloride isomers: *ortho* (**O**), *meta* (**M**), and *para* (**P**).

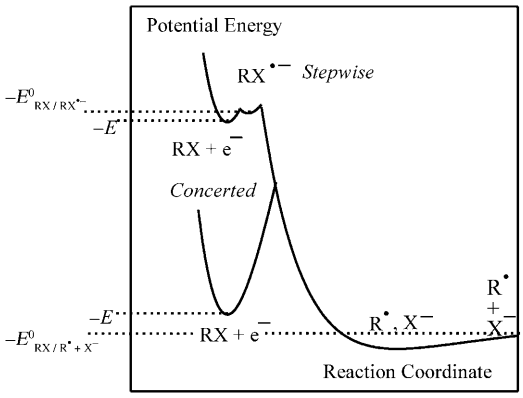

Figure 2. Potential-energy profiles for the concerted and stepwise pathways involving the formation of a σ ion radical according to Scheme 2. The E^0 are the standard potentials of the subscript couples. E is the electrode potential or the standard potential of the homogeneous donor.

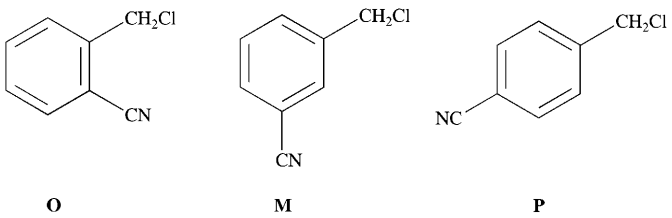

O **M** **P**

Results

All three compounds were investigated by cyclic voltammetry in *N*,*N*-dimethylformamide (DMF) on a glassy carbon electrode. Their low-scan-rate cyclic voltammograms (Figure 3) exhibit two waves, the first of which is bielectronic and irreversible, and the second monoelectronic and reversible. The latter wave corresponds to reversible reduction of the corresponding cyanotoluene. The first wave thus corresponds to reductive cleavage of the starting chloride into a cyanobenzyl radical and a chloride ion. This may occur concertedly or stepwise (Scheme 3). As suggested by the shape of the first wave and potential differences between first and second waves, the compounds fall into two categories: **M** follows a stepwise mechanism, while the **O** and **P** follow a concerted mechanism.

***meta*-Cyanobenzyl chloride**: The first-wave peak potential E_p varies linearly with the logarithm of the scan rate by −50 mV per unit with a peak width of $E_{p/2}-E_p = 80$–110 mV (Figure 4). This behavior is consistent with electron transfer as rate-determining step. In the case of a concerted mechanism, the rate-determining step is necessarily the electron transfer. In the case of a stepwise mechanism, if bond breaking is rate-determining, then $\partial E_p/\partial \log \nu = -30$ mV, whereas

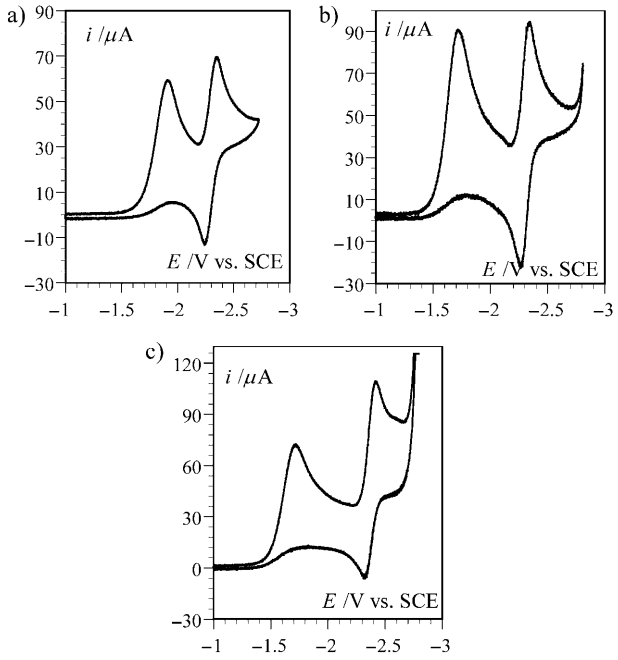

Figure 3. Cyclic voltammetry of the cyanobenzyl chloride isomers in DMF + NBu_4PF_6 (0.1 mol L^{-1}) on a GC electrode in the presence of an acid (phenol). $v = 0.2\ V\,s^{-1}$. a) 2.1 mmol L^{-1} **M**. b) 3.1 mmol L^{-1} **O**. c) 2.4 mmol L^{-1} **P**.

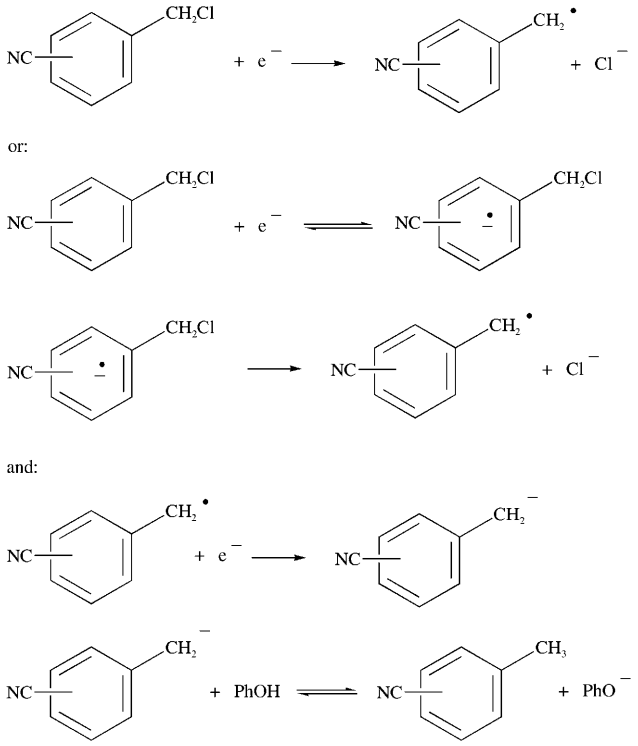

Scheme 3. Reduction mechanism of cyanobenzyl chloride.

if electron transfer is rate-determining, then $\partial E_p/\partial \log v = -29/\alpha$ mV where α is the transfer coefficient. The experimental slope of −50 mV per unit rules out bond breaking as rate-determining step.

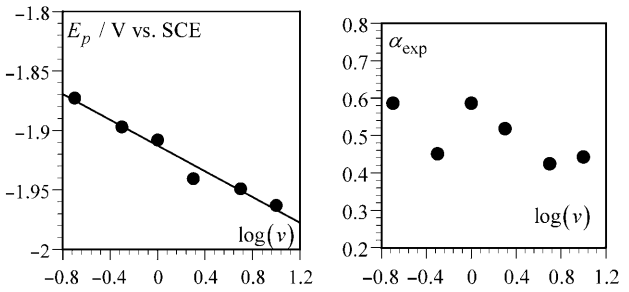

Figure 4. Left: Peak potential as a function of the logarithm of the scan rate (in $V\,s^{-1}$) for **M**. Line: linear fit. Right: Experimental transfer coefficient α_{exp} as a function of the logarithm of the scan rate (in $V\,s^{-1}$) for **M** from Equation (2).

In the framework of an electron-transfer rate-determining step, the experimental value of the transfer coefficient α_{exp} can be calculated from Equation (2).[13]

$$\alpha_{exp} = 1.857\frac{RT}{F}/(E_{p/2} - E_p) \qquad (2)$$

Values close to 0.5 (Figure 4) are obtained. Assuming a concerted dissociative electron-transfer mechanism, the transfer coefficient is given by the dissociative electron-transfer model [Eq. (3)]:[6]

$$\alpha_c = \frac{\partial \Delta G^{\neq}}{\partial \Delta G^0_C} = \frac{1}{2}\left(1 + \frac{E_p - E^0_{RCl/R^{\bullet}+Cl^-}}{\lambda_0 + D_R}\right) \qquad (3)$$

where $\Delta G^{\neq}$ is the activation free enthalpy, $\Delta G^0_C = E_p - E^0_{RCl/R^{\bullet}+Cl^-}$ the standard free enthalpy, λ_0 the solvent reorganization energy, and D_R the C–Cl homolytic bond-dissociation energy. Experimental values of α_{exp} close to 0.5 would indicate that the peak potential is close to the standard potential $E^0_{RCl/R^{\bullet}+Cl^-}$, which can be estimated from Equation (4).

$$E^0_{RCl/R^{\bullet}+Cl^-} = -D_R + T\Delta S_{RCl \rightarrow R^{\bullet}+Cl^{\bullet}} + E^0_{Cl^{\bullet}/Cl^-} \qquad (4)$$

Previous calculations gave $D_R = 2.83$ eV[14] and ab initio calculation[15] leads to $T\Delta S_{RCl \rightarrow R^{\cdot}+Cl^{\cdot}} = 0.302$ eV. The $E^0_{Cl^{\bullet}/Cl^-}$ is 1.81 V versus SCE. It ensues that $E^0_{RCl/R^{\bullet}+Cl^-} = -0.72$ V versus SCE. Since peak potential is around −1.92 V versus SCE, that is, much more negative than $E^0_{RCl/R^{\bullet}+Cl^-}$, the concerted transfer coefficient should be much smaller than 0.5 [Eq. (3)], which is not the case (Figure 4). Consequently, the concerted pathway can be ruled out. We are thus left with a stepwise mechanism and the electron-transfer step as rate-determining step. The transfer coefficient is then given by the Marcus–Hush law [Eq. (5)]:[5]

$$\alpha_s = \frac{\partial \Delta G^{\neq}}{\partial \Delta G^0_S} = \frac{1}{2}\left(1 + \frac{E_p - E^0_{RCl/RCl^{\bullet-}}}{\lambda_0 + \lambda_i}\right) \qquad (5)$$

where $\Delta G^{\neq}$ is the activation free enthalpy, $\Delta G^0_S =$

$E_p - E^0_{RCl/RCl^{\bullet-}}$ the standard free enthalpy, λ_0 the solvent reorganization energy, and λ_i the internal reorganization energy. A transfer coefficient close to 0.5 and a peak potential around −1.92 V versus SCE implies that the standard potential $E^0_{RCl/RCl^{\bullet-}}$ is close to −1.9 V versus SCE.

***ortho*- and *para*-Cyanobenzyl chloride**: In both cases, the first wave is shifted toward more positive potentials as compared to **M**, whereas the second wave remains identical, that is, corresponds to cyanotoluene reduction. Based on the peak-width values one might conclude that electron transfer is rate determining and the experimental transfer coefficient is slightly smaller than 0.5. The shift of the peak potential suggests that the charge-transfer and bond-breaking process are concerted. Since the standard potential $E^0_{RCl/RCl^{\bullet-}}$ is expected to be very close to the value estimated for **M**, that is, −1.9 V versus SCE, the observed peak potential (−1.73 V vs. SCE at 0.2 V s^{-1}, for example) would lead, in the framework of a stepwise mechanism, to a transfer coefficient much larger than 0.5 [Eq. (5)], in contradiction with the experimental peak width, which suggests that a concerted dissociative electron-transfer mechanism is indeed followed by **O** and **P**.

Experimental data were then analyzed in the framework of the concerted dissociative electron-transfer model,[6] for which a quadratic activation/driving force relationship applies [Eq. (6)]

$$\Delta G^{\neq} = \frac{D_{ap} + \lambda_0}{4}\left(1 + \frac{\Delta G^0_C}{D_{ap} + \lambda_0}\right)^2 \qquad (6)$$

where D_{ap} is an apparent bond dissociation energy, whose exact meaning will be discussed below. The experimental data for plotting $\Delta G^{\neq}$ versus ΔG^0 were obtained from the shape and location of the voltammetric waves. The activation free energy at the peak potential was derived according to Equation (7)[6d]

$$\Delta G^{\neq}_p = \frac{RT}{F}\left\{\ln\left(Z^{el}\sqrt{\frac{RT}{\alpha_{exp} F \nu D}}\right) - 0.78\right\} \qquad (7)$$

in which ν is the scan rate, D the diffusion coefficient (taken as equal to 6.7×10^{-5} cm^2 s^{-1}), and α_{exp} the transfer coefficient, which is extracted from the peak width through Equation (2). The pre-exponential factor is taken as equal to the electrochemical collision frequency: $Z_{el} = (\sqrt{RT/2\pi M})$, where M is molar mass.

The experimental standard free energies at the peak were estimated from $\Delta G^0_C = E_p - E^0_{RCl/R^{\bullet}+Cl^-}$) with the standard potential $E^0_{RCl/R^{\bullet}+Cl^-}$ given by Equation (4). Previous calculations gave $D_R = 2.83$ eV, and $T\Delta S_{RCl\rightarrow R^{\bullet}+Cl^{\bullet}}$ was obtained from ab initio calculations. The $\Delta G^{\neq}_p/\Delta G^0_p$ plots were fitted with Equation (6) by using D_{ap} as a fitting parameter. The results are shown in Figure 5 and Table 1.

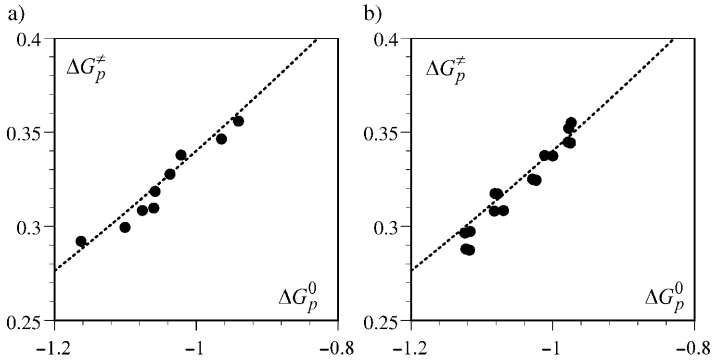

Figure 5. Activation/driving force plots obtained from the variation of the peak potential with the scan rate by using Equation (7). Dotted line: fitting with Equation (6) (parameters from Table 1). a) **O**, (b) **P**.

Table 1. Dissociative electron transfer parameters of **O** and **P**.

	O	**P**
Z^{el} [cm s^{-1}]	5103.9	5103.9
$T\Delta S^0$ [eV]	0.296	0.299
$E^0_{RCl/R^{\bullet}+Cl^-}$ [V]	−0.724	−0.721
λ_0 [eV]	1.05	1.05
D_{ap} [eV]	1.98	1.98
D_R [eV]	2.83	2.83
α_{exp}	0.3–0.4	0.38–0.45

Discussion

Analysis of the experimental data for **M** shows that its standard potential $E^0_{RCl/RCl^{\bullet-}}$ is at least 300 mV more positive than that of the corresponding hydro compound (*meta*-cyanotoluene). In the case of *para*-nitrobenzyl chloride, this difference is less than 200 mV.[16] This indicates that the effect of chlorine on the standard potential is more pronounced for cyano derivatives than for nitro derivatives, in line with the less electro-attractive effect of the cyano group compared to the nitro group. This result is in agreement with previous results obtained with *para*-nitrobenzyl fluoride, for which the standard potential difference between the fluoro and hydro compounds is 300 mV due to the stronger effect of fluorine compared to chlorine.[17] Thus, both the shape and location of the reduction wave of **M** can be explained in the framework of a stepwise dissociative electron-transfer mechanism.

Analysis of the experimental data for **O** and **P** shows that they both follow a concerted mechanism. However, two observations are puzzling. First, application of the dissociative electron-transfer model leads to apparent bond-dissociation energies D_{ap} that are much smaller than the calculated bond-dissociation energies D_R (Table 1). Owing to the quadratic activation/driving force relationship [Eq. (6)], the experimental kinetics is thus faster than predicted by the model. Second, in the framework of a concerted mechanism, transfer coefficients smaller than 0.5 are expected. This is observed experimentally but to a lesser extent than predicted by the model, at least for **P**, the transfer coefficient of

which is close to 0.5 (Table 1). Regarding the first observation, we can at first glance invoke in-cage interactions. As mentioned in the introduction, attractive interactions between the two fragments resulting from cleavage may lead to an ion–radical adduct, which may or may not survive in a polar solvent (Scheme 2). This adduct, resulting from a charge-dipole attractive interaction between the cage fragments before they diffuse out, can be viewed alternatively as a σ anion radical or as forming a weak three-electron bond. Even though such interactions are expected to decrease or even vanish in polar liquid phase, several experimental studies have confirmed their existence, at least when a partial positive charge is induced on the remaining radical part thanks to the presence of strongly electron withdrawing substituents. This is, for example, the case during electrochemical dehalogenation of carbon tetrachloride.[11] Albeit small in magnitude (typically a few tens of meV), these interactions may strongly affect the dynamics of dissociative charge transfer to the parent molecule. If the sticky interaction amounts to about 1% of D_R, then a decrease of about 15% in the intrinsic barrier will ensue,[12] and thus the reaction is accelerated to an experimentally detectable degree. Several experimental works have confirmed the reality of such interactions and the applicability of the model. These examples mostly concerned heterogeneous reactions[18] but examples of homogeneous electron transfer have also been found.[19] Thus, this effect can be considered to be at the origin of the D_{ap} values obtained in this study. The model incorporating such attractive in-cage interactions is referred to as the "sticky dissociative electron transfer model"[11] and leads to Equation (8)

$$D_{R^{\bullet},Cl^{-}\rightarrow R^{\bullet}+Cl^{-}} = (\sqrt{D_R}-\sqrt{D_{ap}})^2 \quad (8)$$

which allows $D_{R^{\bullet},Cl^{-}\rightarrow R^{\bullet}+Cl^{-}} = 0.076$ eV to be estimated for both **O** and **P**. As shown in Scheme 4,[2b] this effect can induce a passage from a stepwise mechanism to a concerted mechanism if the electronic state of the products is modified in such a way that the concerted mechanism becomes energetically more favorable.

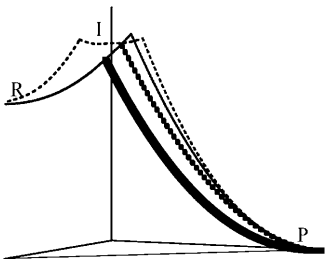

Scheme 4. Three-dimensional representation of the concerted (full lines: thin: without in-cage interactions; thick: with attractive in-cage interactions) and stepwise (dotted lines: thin: without in-cage interactions; thick: with attractive in-cage interactions) reaction pathways. R: reactants ($RX+e^-$); I: intermediate ($RX^{\bullet-}$), P: products ($R^{\bullet}+X^-$).

However, one would then expect stronger in-cage interaction for **P** than for **O** thanks to the larger dipole momentum of the benzylic radical (calculated values are 5.05, 4.77, and 4.61 D for **P**, **O**, and **M**, respectively).[15] If **O** and **P** were involved in in-cage interaction of comparable energy, one would expect an interaction of comparable magnitude for **M**, and thus a concerted mechanism should also be favored. This is not the case. Consequently, this in-cage interaction probably takes place to some extent but cannot explain the passage from a stepwise to a concerted mechanism when changing the position of the cyano substituent on the aromatic ring. The mechanistic shift seems a priori unexpected. All the parameters invoked so far to explain a shift in mechanism [Eq. (1)] are similar among the family of compounds (bond-dissociation energy, entropy of dissociation, standard potential of the leaving group, and in-cage interaction). We are thus left with the following question: why does the mechanism change from a stepwise pathway for **M** to a concerted pathway for **O** and **P**?

In cyclic voltammetry, the peak is reached when the rates of electron transfer and diffusion are equal. Consequently, for the three investigated compounds, the electron-transfer activation energy at the peak potential remains the same at a given scan rate [Eq. (7)]. Therefore, the shift in potential peak observed between **M** and **O**/**P** is a consequence of an energetic shift of the electron-transfer transition state (Scheme 5). This transition state corresponds to the crossing of reactant and product electronic states. It is reasonable to assume that the shape of the reactant energy curve is identical for all three isomers. Thus, an explanation for the change in location of the transition state is to consider an energetic shift of the product electronic-state curve. The reactant energy curve will respond by translating upward so that the activation energy remains the same. This vertical translation is endowed with a peak shift, that is, a change in the energy of the electron being transferred. All of the parameters characterizing the energetic position of the product energy curve (bond-dissociation energy, entropy of dissociation, standard potential of the leaving group, and in-cage interaction) are similar among the family of compounds. Therefore, a nonthermodynamic effect must be invoked to interpret the behavior of **M** on the one hand and **O** and **P** on the other.

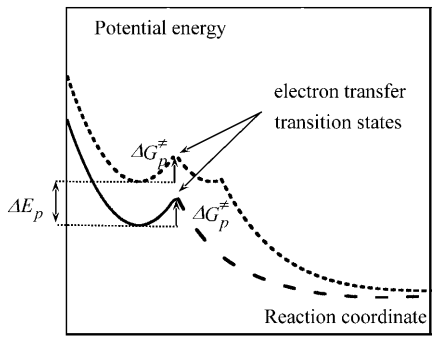

Scheme 5. Schematic representation of peak potential shift due to transition state energetic shift.

Benzylic π anion radicals $^{-\bullet}$RX are intrinsically fragile because the resulting benzylic radical R$^\bullet$ is stabilized thanks to delocalization of the unpaired electron. In other words, contrary to the situation observed with arylic compounds,[7f] the π* orbital receiving the extra electron in the π anion radical $^{-\bullet}$RX does overlap with the σ* C–Cl orbital. Putting this in term of electronic states means that the π* and σ* diabatic states mix. This mixing is expected to be strongly influenced by the nature and the position of substituents on the aromatic ring. Such effects have been previously described through gas-phase quantum calculations on *meta*- and *para*-nitrobenzyl chlorides as well as on *meta*- and *para*-cyanobenzyl bromides.[20] It has been demonstrated that *meta* π anion radicals are less fragile than their *para* isomers, that is, the intrinsic activation barrier is larger in the former case than in the latter. Moreover, EPR studies have shown that in benzonitrile anion radical the hyperfine constants (a direct measure of spin density) are greater at the *para* (8.42 G) and *ortho* (3.63 G) positions than at the *meta* position (0.3 G).[21] Thus, in this anion radical the spin density is essentially zero at the *meta* position, in line with the *meta* position being at the node in the singly occupied molecular orbital. The same is likely to hold true for the cyanobenzyl chloride anion radicals.

Consequently, it can be anticipated that the electronic coupling between the π* and σ* diabatic states is stronger in the case of the **O** and **P** than in **M**. If the coupling is so strong that the π anion radical no longer exists, that is, lives for less than a vibration (Scheme 6), then the concerted pathway is necessarily followed. Since the activation barrier for bond breaking of typical benzylic π anion radicals is small, it is not unrealistic to conceive that such a situation (vanishing of the barrier) may be reached for both **O** and **P**.

How large must this effect be for the $^{-\bullet}$RX cleavage barrier to vanish? To answer this question, the adiabatic electronic state $G_{P,adia}$ of the products was generated by mixing the π* and σ* diabatic states ($G_{\pi,dia}$ and $G_{\sigma,dia}$, respectively) with coupling constant H. It can be shown that the adiabatic electronic state $G_{P,adia}$ of the products is given by Equation (9).[15]

$$G_{P,adia} = \frac{G_{\pi,dia} + G_{\sigma,dia}}{2} - \frac{1}{2}\sqrt{(G_{\sigma,dia} - G_{\pi,dia})^2 + 4H^2} \qquad (9)$$

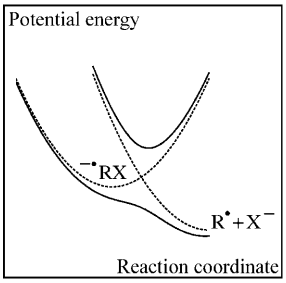

Scheme 6. Diabatic (dotted lines) and adiabatic (full lines) electronic states of the products in the case of strong coupling.

The transition state for electron transfer occurs at the crossing of this adiabatic state with the reactant electronic state $G_{R,dia}$ in a region of phase space in which the π* diabatic state is more stable than the σ* diabatic state. In other words, the weight of the π* diabatic state in the adiabatic state of the products is more important than the weight of the σ* diabatic state. We then assume that the coupling effect remains constant in the phase-space region corresponding to the electron-transfer transition state, that is, the stabilization energy of the adiabatic state toward the π* diabatic state does not significantly depend on the energy difference of the diabatic states $G_{\pi,dia} - G_{\sigma,dia}$. Within this framework, it can be easily shown that the activation/driving force relationship $\Delta G^{\neq} = f(\Delta G^0_C)$ is given by Equation (10)[15]

$$\Delta G^{\neq} = \frac{\lambda_S}{4}\left(1 + \frac{\Delta G^0_C + \Delta E^0 - h}{\lambda_S}\right)^2 \qquad (10)$$

in which λ_S is the reorganization energy corresponding to the stepwise mechanism, $\Delta E^0 = E^0_{RCl/R^\bullet + Cl^-} - E^0_{RCl/RCl^{\bullet -}}$, $\Delta G^0_C = E_P - E^0_{RCl/R^\bullet + Cl^-}$, and h is the gap between the adiabatic state of the products and the π* diabatic state [Eq. (11)].[15]

$$h \approx \frac{H^2}{G_{\sigma,dia} - G_{\pi,dia}} \qquad (11)$$

We can now estimate h from experimental data using Equation (10), $\Delta G^{\neq}$ is derived from Equation (7), $\Delta G^0_C + \Delta E^0 = (E_P - E^0_{RCl/RCl^{\bullet -}})$ is calculated from $E^0_{RCl/RCl^{\bullet -}} = -1.9$ V versus SCE, and λ_S is estimated to be 1.25 eV.[22] We thus obtain $h \approx 0.15$ eV. Therefore $H > 0.15$ eV. This coupling is strong. This is necessary for the vanishing of the bond-breaking activation barrier. Such a situation is sketched in Figure 6. The passage from a stepwise mechanism for **M** to a concerted mechanism for **O** and **P** thus appears as a consequence of a modulation of electronic states coupling on modification of the molecular structure.

From Equation (10), it can be seen that the transfer coefficient α for **O** and **P** is given by Equation (12).

$$\alpha = \frac{\partial \Delta G^{\neq}}{\partial \Delta G^0_C} = \frac{1}{2}\left(1 + \frac{\Delta G^0_C + \Delta E^0 - h}{\lambda_S}\right) \qquad (12)$$

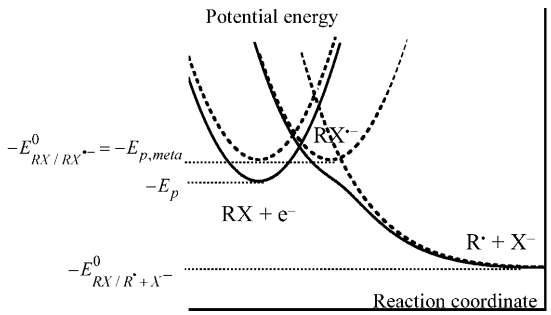

Figure 6. Potential-energy profiles for the stepwise pathway (dotted lines) and concerted pathway (full lines).

Since $\Delta G_C^0+\Delta E^0-h$ is less negative than ΔG_C^0 but more negative than ΔG_S^0, it can be predicted that the transfer coefficient should be larger than expected for a "classical" concerted dissociative electron-transfer mechanism but smaller than for a sequential mechanism, as is indeed observed experimentally.

Previous analyses of the electrochemical and photoinduced reduction of **P** concluded a concerted mechanism with an attractive in-cage ion/radical interaction that can be modulated by the solvent polarity.[4] The present work confirms this mechanism and gives new insights into its origin. The concerted mechanism is not followed because it is more favorable than the stepwise mechanism thanks to the in-cage attractive interaction. If so, one would expect **M** to follow the same concerted mechanism. The concerted mechanism is followed because the π anion radical does not exist for both **O** and **P**, thanks to strong coupling between the π* and σ* electronic diabatic states.

As shown previously,[20b] the very existence of the π anion radical can be due to the solvent. It thus appears that the existence of the π anion radical results from a balance between several effects such as intrinsic barrier for cleavage, solvent polarity (the more polar the solvent, the more stable the π anion radical), and electronic coupling, modulated by the molecular structure. In the case of **M**, the balance is in favor of the π anion radical existing, since in a moderately polar solvent such as acetonitrile, the mechanism is driven toward a stepwise pathway. In the case of **P**, the balance may be reversed, since a concerted mechanism occurs in 1,2-dichloromethane, acetonitrile, *N*,*N*-dimethylformamide, ethanol, and formamide, whereas a stepwise mechanism, with a very fast cleavage step, is observed in water.[9b]

Conclusions

Electrochemical dechlorination of the cyanobenzyl chlorides in DMF leads to the observation of a mechanism shift, depending on the position of the cyano substituent on the aromatic ring. While the reduction of **M** occurs along a two-step pathway, both **O** and **P** are reduced along a concerted pathway via a single transition state. This mechanistic transition results from modulation of the electronic coupling between the diabatic states of the products, which makes the cleavage barrier for both *para* and *ortho* anion radicals disappear. An intermediate anion radical only persists in the case of **M**. This electronic effect appears in addition to the structural parameters (bond-dissociation energy, entropy of dissociation, standard potential of the leaving group, and in-cage interaction between cleaved fragments) that control the occurrence of one (sequential) or the other (concerted) reductive mechanism. It has been semiquantitatively modeled by a modification of the dissociative electron-transfer model, which opens the door to identification and analysis of similar cases.

Experimental Section

Chemicals: *N*,*N*-dimethylformamide (Fluka, >99.5%, stored on molecular sieves and under argon atmosphere), the supporting electrolyte NBu_4PF_6 (Fluka, puriss), *ortho*-cyanobenzyl chloride (Interchim), and *meta*-cyanobenzyl chloride (Chemstep) were used as received.

para-Cyanobenzyl chloride was prepared from the corresponding bromide as follows. *para*-Cyanobenzyl bromide (Aldrich, 99%) was dissolved in an acetone/dichloromethane (50/50) in the presence of a 10-fold excess of tetraethylammonium chloride (Acros, 99%) and the mixture heated to reflux for 1 h. After evaporation of the solvent and addition of diethyl ether, the remaining salt precipitated, and the organic phase was filtered and evaporated. The resulting *para*-cyanobenzyl chloride was recrystallized from pentane/dichloromethane (60/40) mixture to give an 84% yield of pure compound. The structure was checked by elemental analysis and ^{1}H NMR.

Instrumentation: The working electrode was a 3 mm-diameter glassy carbon (GC) disk (Tokai) for experiments carried out at scan rates below 1 $V s^{-1}$. For scan rates above 1 $V s^{-1}$ the working electrode was a 1 mm-diameter GC rod obtained by mechanical abrasion of the original 3 mm-diameter rod. The working electrode was carefully polished and ultrasonically rinsed in absolute ethanol before use. The counterelectrode was a platinum wire, and the reference electrode an aqueous SCE electrode. The potentiostat, equipped with positive feedback compensation and current measurer, used at low or moderate scan rates, was the same as previously described.[23] All experiments were done at 20°C; the double-wall jacketed cell was thermostated by circulation of water.

[1] a) For reviews, see refs. [1b–g]. For additional key references, see refs. [1h–o]. b) "Single Electron Transfer and Nucleophilic Substitution": J.-M. Savéant in *Advances in Physical Organic Chemistry, Vol. 26* (Ed.: D. Bethel), Academic Press, New York, **1990**, pp. 1–130; c) J.-M. Savéant, *Acc. Chem. Res.* **1993**, *26*, 455–461; d) "Electron Transfer, Bond Breaking and Bond Formation": J.-M. Savéant in *Advances in Physical Organic Chemistry, Vol. 35* (Ed.: T. T. Tidwell), Academic Press, New York, **2000**, pp. 117–192; e) F. Maran, D. D. M. Wayner, M. S. Workentin in *Advances in Physical Organic Chemistry, Vol. 36*, (Ed.: T. T. Tidwell), Academic Press, New York, **2001**, pp. 85–116; f) R. A. Rossi, A. B. Pierini, A. B. Penenory, *Chem. Rev.* **2003**, *103*, 71–168; g) C. Costentin, M. Robert, J.-M. Savéant, *Chem. Phys.* **2006**, *324*, 40–56; h) T. M. Vallombroso, W. H. Chapmann, J. N. Narvaez, *Angew. Chem.* **1994**, *106*, 110–113; *Angew. Chem. Int. Ed. Engl.* **1994**, *33*, 73–75; i) P. Maslak, W. H. Chapmann, T. M. Vallombroso, *J. Am. Chem. Soc.* **1995**, *117*, 12373–12379; j) P. Maslak, J. N. Narvaez, T. M. Vallombroso, B. A. Watson, *J. Am. Chem. Soc.* **1995**, *117*, 12380–12389; k) J. M. Tanko, R. E. Drumright, *J. Am. Chem. Soc.* **1990**, *112*, 5362–5363; l) J. M. Tanko, R. E. Drumright, *J. Am. Chem. Soc.* **1992**, *114*, 1844–1854; m) J. M. Tanko, R. E. Drumright, N. K. Suleman, L. E. Brammer, Jr., *J. Am. Chem. Soc.* **1994**, *116*, 1785–1791; n) J. M. Tanko, J. P. Phillips, *J. Am. Chem. Soc.* **1999**, *121*, 6078–6079; o) J. M. Tanko, X. Li, M. Chahma, W. F. Jackson, J. N. Spencer, *J. Am. Chem. Soc.* **2007**, *129*, 4181–4192.

[2] a) This representation is somewhat misleading, since a specific reaction coordinate should be used for each elementary step of the pathways sketched in Scheme 1.[2b] However, this representation is preferred for the sake of simplicity; b) C. Costentin, M. Robert, J.-M. Savéant, *J. Phys. Chem. A* **2000**, *104*, 7492–7501.

[3] a) C. P. Andrieux, J.-M. Savéant, *J. Electroanal. Chem.* **1986**, *205*, 43–58; b) C. P. Andrieux, M. Robert, F. D. Saeva, J.-M. Savéant, *J. Am. Chem. Soc.* **1994**, *116*, 7864–7871; c) L. Pause, M. Robert, J.-M. Savéant, *J. Am. Chem. Soc.* **1999**, *121*, 7158–7159; d) S. Antonello, F. Maran, *J. Am. Chem. Soc.* **1999**, *121*, 9668–9676; e) C. Costentin, P. Hapiot, M. Médebielle, J.-M. Savéant, *J. Am. Chem. Soc.* **1999**, *121*, 4451–4460.

[4] L. Pause, M. Robert, J.-M. Savéant, *J. Am. Chem. Soc.* **2001**, *123*, 4886–4895.

[5] a) R. A. Marcus, *J. Chem. Phys.* **1956**, *24*, 966–978; b) N. S. Hush, *J. Chem. Phys.* **1958**, *28*, 962–972; c) R. A. Marcus, *J. Chem. Phys.* **1965**, *43*, 679–701; d) R. A. Marcus, *Electrochim. Acta* **1968**, *13*, 995–1004; e) N. S. Hush, *Electrochim. Acta* **1968**, *13*, 1005–1023.
[6] a) J.-M. Savéant, *J. Am. Chem. Soc.* **1987**, *109*, 6788; b) J.-M. Savéant, *J. Am. Chem. Soc.* **1992**, *114*, 10595–10602; c) C. P. Andrieux, J.-M. Savéant, C. Tardy, *J. Am. Chem. Soc.* **1998**, *120*, 4167–4175; d) J.-M. Savéant, *J. Phys. Chem. B* **2002**, *106*, 9387–9395.
[7] a) J.-M. Savéant, *J. Phys. Chem.* **1994**, *98*, 3716–3724; b) In the case of aryl anion radicals, the model has been improved by taking into account the role of bond bending, which allows a conical intersection to be avoided.[7c–f] c) D. Laage, I. Burghardt, T. Sommerfeld, J. T. Hynes, *ChemPhysChem* **2003**, *4*, 61–68; d) D. Laage, I. Burghardt, T. Sommerfeld, J. T. Hynes, *J. Phys. Chem. A* **2003**, *107*, 11271–11291; e) I. Burghardt, D. Laage, J. T. Hynes, *J. Phys. Chem. A* **2003**, *107*, 11292–11306; f) C. Costentin, M. Robert, J-M. Savéant, *J. Am. Chem. Soc.* **2004**, *126*, 16051–16057.
[8] Z.-R. Zheng, D. H. Evans, E. S. Soazara Chan-Shing, J. Lessard, *J. Am. Chem. Soc.* **1999**, *121*, 9429–9434.
[9] a) D. Behar, P. Neta, *J. Phys. Chem.* **1981**, *85*, 690–693; b) P. Neta, D. Behar, *J. Am. Chem. Soc.* **1981**, *103*, 103–106; c) J. P. Bays, S. T. Blumer, S. Baral-Tosh, D. Behar, P. Neta, *J. Am. Chem. Soc.* **1983**, *105*, 320–324; d) M. Meot-Ner, P. Neta, *J. Phys. Chem.* **1986**, *90*, 168–173.
[10] C. Costentin, M. Robert, J.-M. Savéant, *J. Am. Chem. Soc.* **2003**, *125*, 105–112.
[11] a) L. Pause, M. Robert, J.-M. Savéant, *J. Am. Chem. Soc.* **2000**, *122*, 9829–9835; b) L. Pause, M. Robert, J.-M. Savéant, *J. Am. Chem. Soc.* **2001**, *123*, 11908–11916.
[12] In both cases, the bond dissociation energies, denoted D, are replaced by $(\sqrt{D}-\sqrt{D_{R^{\bullet},X^{-}\rightarrow R^{\bullet}+X^{-}}})^2$, which leads to a substantial lowering of the barrier even for small values of $D_{R^{\bullet},X^{-}\rightarrow R^{\bullet}+X^{-}}$.
[13] J.-M. Savéant in *Elements of Molecular and Biomolecular Electrochemistry*, Wiley-Interscience, New York, **2006**, p. 53.
[14] D. A. Pratt, J. S. Wright, K. U. Ingold, *J. Am. Chem. Soc.* **1999**, *121*, 4877–4882.
[15] See the Supporting Information.
[16] C. P. Andrieux, A. Le Gorande, J.-M. Savéant, *J. Am. Chem. Soc.* **1992**, *114*, 6892–6904.
[17] C. P. Andrieux, C. Combellas, F. Kanoufi, J.-M. Savéant, A. Thiébault, *J. Am. Chem. Soc.* **1997**, *119*, 9527–9540.
[18] a) A. Cardinale, A. A. Isse, A. Gennaro, M. Robert, J.-M. Savéant, *J. Am. Chem. Soc.* **2002**, *124*, 13533–13539; b) C. Costentin, C. Louault, M. Robert, A.-L. Teillout, *J. Phys. Chem. A* **2005**, *109*, 2984–2990.
[19] a) C. Costentin, P. Hapiot, M. Médebielle, J.-M. Savéant, *J. Am. Chem. Soc.* **2000**, *122*, 5623–5635; b) A. A. Isse, A. Gennaro, *J. Phys. Chem. A* **2002**, *108*, 4180–4186.
[20] a) See Figure 3 in ref. [20b]; b) C. Costentin, M. Robert, J.-M. Savéant, *J. Am. Chem. Soc.* **2004**, *126*, 16834–16840.
[21] P. H. Rieger, I. Bernal, W. H. Reinmuth, G. K. Fraenkel, *J. Am. Chem. Soc.* **1963**, *85*, 683–690.
[22] For **M**: $\Delta G^{+}_{p,meta}=(\lambda_S/4)(1+\Delta G^{0}_{p,meta}/\lambda_S)^2$. Since the transfer coefficient is close to 0.5, $\Delta G^{0}_{p,meta}\approx 0$ and thus $\lambda_S\approx 4\Delta G^{+}_{p,meta}\approx 1.25$ eV.
[23] D. Garreau, J.-M. Savéant, *J. Electroanal. Chem.* **1972**, *35*, 309.

Received: June 23, 2008
Revised: September 1, 2008
Published online: November 28, 2008

